Apolipoprotein E Receptor 2 Deficiency Decreases Endothelial Adhesion of Monocytes and Protects Against Autoimmune Encephalomyelitis

Laurent Calvier, Ph.D.[1,2,*], **Navid Manouchehri, M.D.**[3], **Anastasia Sacharidou, Ph.D.**[4], **Chieko Mineo, Ph.D.**[4], **Philip W. Shaul, M.D.**[4], **David Y. Hui, Ph.D.**[5], **Maria Z Kounnas, Ph.D.**[6], **Olaf Stüve, M.D., Ph.D.**[3,7], **Joachim Herz, M.D.**[1,2,3,8,*]

[1] Department of Molecular Genetics, University of Texas (UT) Southwestern Medical Center, Dallas, TX, USA.

[2] Center for Translational Neurodegeneration Research, UT Southwestern Medical Center, Dallas, TX, USA.

[3] Department of Neurology, UT Southwestern Medical Center, Dallas, TX, USA.

[4] Center for Pulmonary and Vascular Biology, Department of Pediatrics, UT Southwestern Medical Center, Dallas, TX, USA.

[5] Department of Pathology, College of Medicine, University of Cincinnati, Cincinnati, OH, USA

[6] Reelin Therapeutics, Inc. La Jolla, CA, USA

[7] Department of Neurology, VA North Texas Health Care System, Medical Service, Dallas, TX, USA.

[8] Department of Neuroscience, UT Southwestern Medical Center, Dallas, TX, USA.

Abstract

Under normal conditions, the blood–brain barrier effectively regulates the passage of immune cells into the central nervous system (CNS). However, under pathological conditions like multiple sclerosis (MS), leukocytes, especially monocytes, infiltrate the CNS where they promote inflammatory demyelination resulting in paralysis. Therapies targeting the immune cells directly and preventing leukocyte infiltration exist for MS but may compromise the immune system. Here,

we explore how apolipoprotein E receptor 2 (ApoER2) regulates vascular adhesion and infiltration of monocytes during inflammation. We induced experimental autoimmune encephalitis (EAE) in ApoER2 knockout mice, and in mice carrying a loss-of-function mutation in the ApoER2 cytoplasmic domain. In both models, paralysis and neuroinflammation were largely abolished as a result of greatly diminished monocyte adherence due to reduced expression of adhesion molecules on the endothelial surface. Our findings expand our mechanistic understanding of the vascular barrier, the regulation of inflammation and vascular permeability, and the therapeutic potential of ApoER2-targeted therapies.

ONE-SENTENCE SUMMARY

Loss of ApoER2 reduces endothelial adhesion and monocyte extravasation, thereby reducing neuroinflammation, paralysis and mortality.

INTRODUCTION

Chronic inflammation and excessive recruitment of circulating leukocytes (1, 2) is an early event and a key mechanism in several diseases including multiple sclerosis (MS). The endothelium functions as a barrier between the circulation and the extravascular space, which protects the tissues from inappropriate attack by the body's own immune system. Extravasation of immune cells proceeds in two steps and requires first endothelial adhesion followed by endothelial transmigration. Both steps are primarily regulated by NF-κB target genes (3, 4). Although the trigger for MS remains elusive, key insights have been gleaned that allow us to better understand the autoimmune response. Monocytes infiltrate the nervous system in MS, causing inflammatory demyelination (2), and subsequent paralysis (5). For instance, the deletion of the chemokine receptor CCR2 from inflammatory monocytes inhibits paralysis in a mouse model (1) of MS, indicating that blocking monocyte extravasation is sufficient to prevent MS. Based on this paradigm, many disease-modifying agents (DMA) approved for relapsing forms of MS target the immune system to block the infiltration of leukocytes, such as natalizumab, a monoclonal antibody that binds to α4-integrin on the leukocytes and prevents their infiltration into the central nervous system (CNS) (6, 7). However, medications that mitigate inflammation in a variety of diseases, including MS, may also compromise the immune system. For example, natalizumab is associated with greatly increased risk of progressive multifocal leukoencephalopathy (PML), a viral infection of the brain that is often fatal (8). Therefore, more options for modulating vascular permeability of monocytes is required to identify superior non-immunosuppressive therapeutic targets.

Apolipoprotein E receptor 2 (ApoER2) encoded by the *Lrp8* gene is a member of the LDL receptor gene family and expressed on the surface of vascular endothelial cells where it regulates leukocyte-endothelial cell adhesion (9, 10). ApoER2 deletion in mice reduces leukocyte-endothelial cell adhesion in response to antiphospholipid antibodies (9, 11). Therefore, ApoER2 appears to regulate leukocyte adhesion to the endothelium, but its role in chronic inflammatory diseases, such as MS, remains to be determined.

In this study, we explore a non-immunosuppressive mechanism that regulates vascular adhesion and extravasation of monocytes. We hypothesized that ApoER2 signaling in endothelial cells is required for monocyte adhesion and extravasation during chronic inflammatory diseases, such as MS. To test this hypothesis, we used ApoER2 KO mice (12) and ApoER2-EIG mutant mice in which the adapter protein interacting NFDNPVY motif in the cytoplasmic domain of ApoER2 were altered to EIGNPVY which disrupts the ApoER2-Dab1/2 interaction (13, 14) and thus impairs ApoER2 signaling and function (15, 16). *Cx3cr1-GFP* mice, which genetically express GFP in circulating monocytes, were used to monitor the adhesion and infiltration of this inflammatory cell population, which is a pivotal event in the development of MS (1).

RESULTS

ApoER2 KO mice are protected from paralysis.

Experimental autoimmune encephalomyelitis (EAE) (17) is a widely used model for human MS. EAE was induced by immunization with myelin oligodendrocyte glycoprotein (MOG) in littermate ApoER2 wild type (WT) and KO mice (Figure 1A). Paralysis occurred in 64% of the WT mice and was significantly reduced to 18% in the KO (Figure 1B). WT mice developed progressive paralysis starting at the tail at day 13 and reaching a plateau (with slower progression after the exponential phase) at day 18 (Figure 1C). Blinded clinical EAE scoring correlated with decreased body weight (Figure 1D) and inverted hanging time on a grid (Figure 1E), independently reflecting both paresis and paralysis. The EAE index (Figure 1C) was calculated by numerical addition of the EAE clinical scores for each mouse. The same calculation was done for the hanging time index (Figure 1E). Based on the same principle, a weight loss index (Figure 1D) was calculated as the sum of the daily weight losses. For each day, weight loss was defined as the average weight before EAE onset (from day 7 to 10) minus the current weight. Compared to the WT, the ApoER2 KO mice exhibited substantially milder paralysis as indicated by the reduced EAE score, weight loss and hanging time (Figure 1C–E).

These mitigated clinical parameters were accompanied by decreased neuroinflammation (Figure 1F). Both infiltrating monocytes/macrophages and microglia can express Mac-3 (or CD107b), so the microglia-specific marker ionized calcium binding adaptor molecule 1 (Iba1) was used to discriminate between the two populations. ApoER2 KO mice showed a significant reduction of infiltrating monocytes/macrophages (positive for Mac-3, negative for Iba1; Figure 1F). This decreased cell infiltration in ApoER2 KO mice was associated with a strong reduction of endothelial adhesion marker expression, as judged by E-selectin and intercellular adhesion molecule-1 (ICAM-1) in the spinal cord (Figure 1G). In addition, plasma Netrin-1 (an anti-inflammatory marker) level was increased in the KO while the ApoER2 ligand (Reelin) remained unaffected by the mutation (Figure 1G).

ApoER2 KO mice have reduced leukocyte adhesion to endothelium.

Progression of MS depends on monocyte extravasation and infiltration into the CNS (1). To understand the role of ApoER2 in MS progression, we hypothesized that ApoER2 promotes monocyte rolling and adhesion to the vascular wall, the first step toward monocyte

extravasation and inflammation of the CNS. To test this, ApoER2 KO mice were injected with Rhodamine 6G to label leukocytes, followed by intravital microscopy to monitor leukocyte rolling on the vessel wall (Supplementary Movie S1). The number of rolling leukocytes was greatly reduced and rolling velocity was increased in ApoER2 KO mice (Figure 1H). This resulted in decreased leukocyte interaction with the vascular wall as shown by decreased rolling index and cumulative fluorescence signal (illustrated by representative cumulative pictures; Figure 1H), meaning that monocytes are less likely to roll and adhere to the vascular wall, which prevents their infiltration into the surrounding tissues. We did not observe differences between the sexes (Supplementary Figure S1A); white blood cell counts and vessel areas measured by intravital microscopy were similar in both groups (Supplementary Figure S1B).

That the reduced leukocyte rolling and endothelial adhesion was specifically caused by loss of ApoER2 in the endothelium and not a secondary global consequence of systemic ApoER2 deficiency was further confirmed by endothelial cell-specific deletion of this receptor (Supplementary Figure S2). Taken together, these observations indicate that ApoER2 regulates endothelial adhesion properties in an endothelial cell-specific manner.

ApoER2 loss-of-function protects from neuroinflammation and paralysis.

We next explored whether a loss of function mutation in ApoER2 (EIG, Figure 2A) which prevents the interaction of ApoER2 with the cytoplasmic signal transducing adapter proteins Dab1/2, would have a similar effect. EAE was induced in mice harboring genetically labeled, GFP-expressing monocytes (*Cx3cr1-GFP*). Approximately 50% of the WT animals died, whereas only 7% in the ApoER2 mutant group succumbed to the disease (Figure 2B). In this second model, WT mice developed progressive ascending paralysis starting at day 12 and reaching a plateau at day 17 (Figure 2C), accompanied by substantial weight loss (Figure 2D) and decreased hanging time (Figure 2E). EAE, weight and hanging time recovery scores were calculated for each mouse as the difference between the maximum (for EAE score) or minimum (for weight and hanging time) and the endpoint at day 21. Compared to WT, ApoER2 mutant mice exhibited less paralysis. The maximal EAE score overall was lower and was reached at day 16, followed by a remission phase. At the end of the 21-day duration of the experiment, the EAE score was on average 3 points lower than in the WT group (Figure 2C). There was no difference in the loss of body weight (Figure 2D), but hanging time, and thus grip strength, was also improved (Figure 2E). These mitigated clinical parameters were accompanied by decreased neuroinflammation (Figure 3A) and accumulation of inflammatory cells (Figure 3B) in the spinal cord of the mutant mice. Both resident microglia and infiltrating monocytes expressed *Cx3cr1*-GFP, so the microglia-specific marker Iba1 was used to discriminate between the two populations. ApoER2 mutant mice showed a significant reduction of total inflammatory cell number (positive for *Cx3cr1*-GFP, regardless of Iba1 expression) and infiltrating monocytes (positive for *Cx3cr1*-GFP, negative for Iba1; Figure 3B). Importantly, leukocyte (especially T cell) activation was not affected by the ApoER2 mutation during the early stages of EAE (Supplementary Figure S3B), suggesting that the differences observed between genotypes are driven by endothelial cells.

ApoER2 loss-of-function reduces vascular adhesion of leukocytes.

We hypothesized that the reduced infiltration of monocytes would be accompanied by the downregulation of endothelial adhesion marker expression, especially E-selectin, a major adhesion protein responsible for monocyte rolling. In our ApoER2-EIG mice, plasma Netrin-1 (an anti-inflammatory marker) level was increased while E-selectin and ICAM-1 expression in the total spinal cord was decreased (Figure 3C). This raises the possibility that loss of function of ApoER2 decreases monocyte adhesion and rolling not only through reduced direct activation of NF-κB signaling, but also through a concomitant increase of Netrin-1 expression.

To confirm that ApoER2 loss of function reduces monocyte adhesion *in vivo*, we performed intravital microscopy to monitor monocyte rolling on the vessel wall of *Cx3cr1-GFP*, ApoER2-EIG mice (Supplementary Movie S2). The number of GFP-labeled rolling monocytes was greatly reduced and rolling velocity was increased in ApoER2-deficient mice (Figure 4A). This resulted in decreased monocyte exposure to the vascular wall as shown by decreased rolling index and cumulative GFP-intensity (illustrated by representative cumulative pictures; Figure 4A). As with the rhodamine-labeled leukocytes, we did not observe sex-related differences in monocyte adhesion or velocity (Supplementary Figure S1C). Neither was white blood cell count affected by the mutation (Supplementary Figure S1D), and the vessel area measured by intravital microscopy was similar in both groups (Supplementary Figure S1D). In accordance with our previous results, we observed that impaired Reelin/ApoER2 signaling in ApoER2 mutant mice increased anti-inflammatory Netrin-1 levels in the plasma (Figure 4B) and decreased E-selectin expression in the aorta (Figure 4C).

DISCUSSION

Based on the above literature and our current work, we suggest that activation of ApoER2 by Reelin increases adhesion molecule expression on the vascular endothelium in an NF-κB dependent manner, thereby promoting the rolling, adhesion, and extravasation of monocytes. In the context of MS, this infiltration of monocytes into the CNS leads to myelin degradation and subsequent paralysis. Conversely, ApoER2 deletion or loss of function reduces endothelial adhesion and extravasation of monocytes, thereby dampening nervous system inflammation, reducing paralysis and mortality, as well as improving recovery. This proposed mechanism is illustrated in Figure 4D. While this focused study has provided new insights into ApoER2 function in the endothelium during inflammation, we cannot exclude non-vascular effects that could conceivably contribute to the protective effect.

We have previously published a role in vascular adhesion for plasma Reelin (18, 19), a primary ApoER2 ligand (10). Reelin is increased by two-fold in the serum of MS patients, resulting in increased endothelial adhesion of leukocytes through increased NF-κB-mediated expression of vascular adhesion molecules (10, 18, 19). We have also investigated the prophylactic and therapeutic potential of Reelin depletion in EAE and further validated the results in Reelin conditional KO mice (18). Removal of plasma Reelin by either approach protected against neuroinflammation and largely abolished the neurological consequences by reducing endothelial permeability and immune cell accumulation in the CNS. The present

study on the Reelin receptor ApoER2 confirm and extend these results, highlighting a role for the Reelin-ApoER2 pathway in vascular adhesion, inflammation and MS.

In accordance with the literature, our results suggest antinomic roles for Reelin and Netrin-1. Reelin and Netrin-1 are two plasma proteins that were both originally identified for their roles in neuronal migration and axon guidance during neurodevelopment. Both were recently reported to differentially regulate adhesion markers (E-selectin, ICAM-1, and vascular cell adhesion molecule-1 (VCAM-1)) on endothelial cells (10, 20). While Reelin binding to endothelial ApoER2 activates the NF-κB pathway and thus promotes the expression of endothelial-leukocyte adhesion markers (10), Netrin-1 by contrast binds to its receptor Unc5b and inhibits NF-κB signaling, thereby decreasing the expression of adhesion markers (20, 21). Therefore, Reelin signaling through ApoER2 is proinflammatory whereas Netrin-1 signaling through Unc5b is anti-inflammatory and inhibits the adhesion and the recruitment of leukocytes (20, 21).

The use of mice with global ApoER2 mutations in this study could constitute a limitation to the interpretation of our results. To exclude any major effect of this mutation on leukocytes (especially T cells), we have validated that their activation was not affected at early EAE stages. To further strengthen this finding, we have also validated in mice with endothelial-specific deletion of ApoER2 that leukocyte rolling and adhesion on the vascular wall were reduced. These results suggest that the differences observed between genotypes are mainly driven by endothelial cells, even if additional effects of ApoER2 mutations in other cell types cannot be completely excluded. Moreover, although we have focused here primarily on monocytes, we have previously shown that ApoER2 mutations affect the adhesion of all leukocytes (10).

In conclusion, our studies have revealed a non-immunosuppressive mechanism that can be therapeutically targeted to reduce vascular adhesion and leukocyte extravasation. This novel concept may lead to innovative therapeutic strategies not only for MS, but also other chronic inflammatory diseases such as atherosclerosis, arthritis or Crohn's disease.

MATERIALS AND METHODS

Study design.

The purpose of this study was to explore a novel pathway regulating endothelial adhesion and permeability to prevent monocyte extravasation instead of directly targeting the immune system. We hypothesized that ApoER2 signaling in endothelial cells is required for monocyte adhesion and extravasation during chronic inflammatory diseases, such as MS. This question was addressed using mouse models for intravital microscopy and EAE. Power analysis was used to determine a range for the sample size and no outliers were excluded. Animals were randomized and EAE was evaluated by two blinded operators. Biological replicates are specified in each figure legend.

Mouse models.

ApoER2 KO have been described previously (12). *Cx3cr1*-GFP mice (B6.129P-Cx3cr1[tm1Litt]/J) were purchased from the Jackson Laboratories (Stock No. 005582). These

mice express EGFP in monocytes, dendritic cells, NK cells, and brain microglia under the control of the endogenous *Cx3cr1* locus. *Cx3cr1*-GFP monocytes downregulate GFP expression upon differentiation into macrophages. ApoER2 EIG (*Lrp8*[tm4Her] obtained previously (13)) and *Cx3cr1*-GFP mice were crossed. *VE-Cad-Cre*; *Lrp8*^{fl/fl} mice (EC-ApoER2 KO) were described previously (16). All animal studies were approved and performed according to the institutional animal care and use guidelines.

Intravital microscopy for quantification of monocyte–endothelial cell adhesion.

Mesenteric vessels are easy to expose and visualize, but this procedure has to be performed on very young mice (typically 4–5 weeks) otherwise the adipose tissue surrounding the vessels makes the imaging impossible due to its autofluorescence. After anesthesia with ketamine/xylazine, the mesentery of 4-week-old mice was exposed for observation and recording of images of GFP-monocyte (or Rhodamine 6G labeled leukocyte) adhesion and rolling using a Retiga digital camera (QImaging) attached to a Nikon Eclipse Ti microscope with NIS Element image-capturing software. For each mouse, videos on 6 different marginal mesenteric veins were recorded. The velocity and quantity of monocyte rolling were measured by ImageJ (wrmtrck plugin) on each video for 10 seconds. The rolling index was calculated as monocyte number / velocity for each record. For each 10-second video, all the frames were stacked into one final picture and the intensity was measured to visually reflect and measure the monocyte exposition to the vascular wall.

After recording, the mice were sacrificed, blood was collected for white blood cell count and plasma analysis, the thoracic aorta was dissected out, the adventitia was removed and the media-intima was snap frozen for further protein analysis.

Experimental autoimmune encephalitis (EAE) model.

Eight-week-old male mice were immunized by subcutaneous injection of myelin peptide MOG35–55 (200μg; Sigma-Aldrich; M4939) in 200μl of emulsified complete Freund's adjuvant (Sigma-Aldrich; F5506) containing 2mg/ml of *Mycobacterium tuberculosis* (Fischer Scientific; DF3114-33-8). In addition, 400ng of pertussis toxin (Fisher Scientific; NC9282261) was administered intraperitoneally on the day 0 and day 2.

EAE severity was blindly evaluated daily from day 7 by survival, EAE clinical score (from 0=healthy to 10=dead) (17), weight loss and hanging test (inverted grid (8×8mm) test for a maximum time of 180 sec). Of note, animals reaching a moribund state were euthanized according to IACUC requirements. An EAE index was calculated by numerical addition of the daily EAE clinical scores over the course of the experiment for each mouse. The same calculation was done for the hanging time index. Based on the same principle, the weight loss index was calculated as the sum of the daily weight loss compared to the average weight of the mouse before onset of EAE symptoms (from day 7 to 12).

At day 21, the mice were sacrificed, blood was collected for plasma analysis, the spinal cord was extracted by hydraulic pressure and cut in 3 pieces (sublumbar and subcervical parts for histology; the thoracic section for protein analysis).

Immunofluorescence.

Tissues were fixed overnight in 4% paraformaldehyde and then cryoprotected in sucrose solutions (15%, then 30% in PBS) followed by embedding in OCT (Tissue-Tek; 4583) and frozen at −80°C. 10-μm-thick cryosections were cut using a Cryostat (Leica). Sections were thawed, re-hydrated in PBS, blocked 1h at room temperature with blocking buffer (1% BSA and 0.03% Tritin-X100 in PBS), incubated with primary antibody (Iba1, Novus Biologicals, NB100-1028) overnight at 4°C in a humid chamber, washed with PBS, incubated with Alexa594-conjugated secondary antibody (anti-goat, Molecular Probes, A11058) 1h at room temperature, washed and mounted using VECTASHIELD antifade mounting medium with DAPI (Vector, H-1200). Images were acquired with a Zeiss Axiophot microscope with AxioVision software and analyzed with ImageJ.

Western blot.

Tissue pieces were prepared by adding protease and phosphatase inhibitor cocktail in RIPA buffer and centrifuging for 10 minutes at 12000x rpm to remove debris. Western blot was performed as previously described (22–24). From the lysates, protein concentrations were determined by the Lowry protein assay (500–0113, 500–0114, 500–0115; Bio-Rad). Equal amounts of protein were loaded into each lane of a 4–12% Tris gel (BioRad) and subjected to electrophoresis. After blotting, nitrocellulose-membranes (BioRad) were blocked for 1h (milk powder 5% in TBS/Tween 0.1–0.2%) and incubated with primary antibodies (ICAM-1, R&D Systems, AF796; E-Selectin, Santa Cruz, sc-137054; G10 anti-Reelin, made in-house; Reelin, Millipore, MAB5366; ApoER2, made in-house; GAPDH, Sigma-Aldrich, G8795; α-Tubulin, Millipore, CP08). Binding of secondary HRP-antibodies were visualized by ECL or ECL plus chemiluminescent (Amersham). After densitometric analyses with ImageJ, optical density values were expressed as arbitrary units and normalized for protein loading, as described in the figure legends.

Lymph node mononuclear cell isolation and Flow cytometry.

The overall percentage of CD4 T helper cell subsets was calculated using multi parameter flow cytometry. Cells from lymph nodes dissected from actively immunized mice at day 13 post immunization were isolated by pressing through a 70 μm nylon mesh cell retainer. Cells were treated with red blood cell (RBC) lysis buffer (Sigma-Aldrich, St. Louis, MO, USA), washed twice with cold phosphate buffered saline (PBS), and resuspended in PBS for counting by hemocytometer. A total of 1×10^6 mononuclear cells were stained. Cells were washed using 2% FBS-PBS (FACS buffer) at 1500 rpm for 5 minutes, followed by incubation with 1 μg Fc Block (anti-CD16/32, Tonbo Biosciences) for 15 minutes at 4°C. Cells were then stained for surface markers using antibodies against CD45 (Alexa Flour 700; Biolegend Clone: 30-F11), CD3 (Pacific Blue; Biolegend Clone: 17A2), and CD4 (PE; Biolegend Clone: GK1.5) for 45 minutes at 4°C and washed with 2% FBS-PBS. Subsequently, cells were stained for intracellular cytokines. Briefly, cells were fixed using fixation buffer (Biolegend, Cat# 420801) and incubated in the dark for 20 minutes. The cells were then pelleted and re-suspended in permeabilization wash buffer (Biolegend, Cat#: 421002) and incubated in the dark for a second time for 15 minutes. Intracellular cytokines were stained in the dark using antibodies against the following cytokines: IFNγ

(PerCP-Cy5.5; Biolegend Clone: XMG1.2), IL-17 (FITC; Biolegend Clone:TC11-18H10.1) and IL-4 (APC; BD Pharmingen Cat#: 554436) for 45 minutes at room temperature. Stained cells were washed with permeabilization wash buffer two more times and resuspended in 2% FBS-PBS for flow cytometry. Events were recorded via BD FACS LSR Fortessa (The Moody Foundation Flow Cytometry Facility, UT Southwestern), equipped with Diva acquisition software (BD Bioscience). Cells were gated according to morphology side scatter (SSC-A) vs forward scatter (FSC-A). Doublets were excluded (FSC-A vs FSC-H and SSC-A vs SSC-H). CD45+ CD3+ CD4+ T helper cells were gated. CD4+ T cell subsets were characterized as IL-17 hi, IL-4 hi or IFNγ hi. In each sample a minimum of 2×10^4 live events were recorded. FlowJo software (BD Biosciences) was used for data analysis.

Statistics.

For animals, the "n" values are specified in each legend. GraphPad Prism was used to run all the statistical analysis. Values from multiple experiments are expressed as mean ± SEM. Normality was tested using the Kolmogorov-Smirnov test. Statistical significance was determined for multiple comparisons using one-way analysis of variance (ANOVA) followed by Tukey multiple comparison (for normal distribution) or Kruskal-Wallis (for non-normal distribution) test. Student's t-test (for normal distribution) or Mann Whitney (for non-normal distribution) was used for comparisons of two groups. To compare the changes between 2 groups over time, a 2-way ANOVA was used. The occurrence/survival curves were tested with Log-rank (Mantel-Cox test). $p<0.05$ was considered significant.

Supplementary Material

Refer to Web version on PubMed Central for supplementary material.

ACKNOWLEDGMENTS

FUNDING

## DATA AND MATERIALS AVAILABILITY

All data associated with this study are present in the paper or the Supplementary Materials. The mouse models used in this study are available through an MTA.

REFERENCES AND NOTES

1. Ajami B, Bennett JL, Krieger C, McNagny KM, Rossi FMV, Infiltrating monocytes trigger EAE progression, but do not contribute to the resident microglia pool, Nat. Neurosci. 14, 1142–1149 (2011). [PubMed: 21804537]

2. Falcão AM, van Bruggen D, Marques S, Meijer M, Jäkel S, Agirre E, Samudyata null, Floriddia EM, Vanichkina DP, Ffrench-Constant C, Williams A, Guerreiro-Cacais AO, Castelo-Branco G, Disease-specific oligodendrocyte lineage cells arise in multiple sclerosis, Nat. Med. 24, 1837–1844 (2018). [PubMed: 30420755]

3. Madonna R, De Caterina R, Relevance of new drug discovery to reduce NF-κB activation in cardiovascular disease, Vascul. Pharmacol. 57, 41–47 (2012). [PubMed: 22366375]

4. Min J-K, Kim Y-M, Kim SW, Kwon M-C, Kong Y-Y, Hwang IK, Won MH, Rho J, Kwon Y-G, TNF-related activation-induced cytokine enhances leukocyte adhesiveness: induction of ICAM-1 and VCAM-1 via TNF receptor-associated factor and protein kinase C-dependent NF-kappaB activation in endothelial cells, J. Immunol. 175, 531–540 (2005). [PubMed: 15972689]

5. Epelman S, Lavine KJ, Randolph GJ, Origin and functions of tissue macrophages, Immunity 41, 21–35 (2014). [PubMed: 25035951]

6. Stüve O, Marra CM, Jerome KR, Cook L, Cravens PD, Cepok S, Frohman EM, Phillips JT, Arendt G, Hemmer B, Monson NL, Racke MK, Immune surveillance in multiple sclerosis patients treated with natalizumab, Ann. Neurol. 59, 743–747 (2006). [PubMed: 16634029]

7. Stüve O, Marra CM, Bar-Or A, Niino M, Cravens PD, Cepok S, Frohman EM, Phillips JT, Arendt G, Jerome KR, Cook L, Grand'Maison F, Hemmer B, Monson NL, Racke MK, Altered CD4+/CD8+ T-cell ratios in cerebrospinal fluid of natalizumab-treated patients with multiple sclerosis, Arch. Neurol. 63, 1383–1387 (2006). [PubMed: 17030653]

8. Cutter GR, Stüve O, Does risk stratification decrease the risk of natalizumab-associated PML? Where is the evidence?, Mult. Scler. 20, 1304–1305 (2014). [PubMed: 24812045]

9. Ramesh S, Morrell CN, Tarango C, Thomas GD, Yuhanna IS, Girardi G, Herz J, Urbanus RT, de Groot PG, Thorpe PE, Salmon JE, Shaul PW, Mineo C, Antiphospholipid antibodies promote leukocyte-endothelial cell adhesion and thrombosis in mice by antagonizing eNOS via β2GPI and apoER2, J. Clin. Invest. 121, 120–131 (2011). [PubMed: 21123944]

10. Ding Y, Huang L, Xian X, Yuhanna IS, Wasser CR, Frotscher M, Mineo C, Shaul PW, Herz J, Loss of Reelin protects against atherosclerosis by reducing leukocyte-endothelial cell adhesion and lesion macrophage accumulation, Science Signaling 9, ra29–ra29 (2016). [PubMed: 26980442]

11. Romay-Penabad Z, Aguilar-Valenzuela R, Urbanus RT, Derksen RHWM, Pennings MTT, Papalardo E, Shilagard T, Vargas G, Hwang Y, de Groot PG, Pierangeli SS, Apolipoprotein E receptor 2 is involved in the thrombotic complications in a murine model of the antiphospholipid syndrome, Blood 117, 1408–1414 (2011). [PubMed: 21119114]

12. Trommsdorff M, Gotthardt M, Hiesberger T, Shelton J, Stockinger W, Nimpf J, Hammer RE, Richardson JA, Herz J, Reeler/Disabled-like disruption of neuronal migration in knockout mice lacking the VLDL receptor and ApoE receptor 2, Cell 97, 689–701 (1999). [PubMed: 10380922]

13. Beffert U, Durudas A, Weeber EJ, Stolt PC, Giehl KM, Sweatt JD, Hammer RE, Herz J, Functional dissection of Reelin signaling by site-directed disruption of Disabled-1 adaptor binding to apolipoprotein E receptor 2: distinct roles in development and synaptic plasticity, J. Neurosci. 26, 2041–2052 (2006). [PubMed: 16481437]

14. Beffert U, Nematollah Farsian F, Masiulis I, Hammer RE, Yoon SO, Giehl KM, Herz J, ApoE receptor 2 controls neuronal survival in the adult brain, Curr. Biol. 16, 2446–2452 (2006). [PubMed: 17174920]

15. Trotter JH, Klein M, Jinwal UK, Abisambra JF, Dickey CA, Tharkur J, Masiulis I, Ding J, Locke KG, Rickman CB, Birch DG, Weeber EJ, Herz J, ApoER2 function in the establishment and maintenance of retinal synaptic connectivity, J. Neurosci. 31, 14413–14423 (2011). [PubMed: 21976526]

16. Sacharidou A, Chambliss KL, Ulrich V, Salmon JE, Shen Y-M, Herz J, Hui DY, Terada LS, Shaul PW, Mineo C, Antiphospholipid antibodies induce thrombosis by PP2A activation via apoER2-Dab2-SHC1 complex formation in endothelium, Blood 131, 2097–2110 (2018). [PubMed: 29500169]

17. Bittner S, Afzali AM, Wiendl H, Meuth SG, Myelin oligodendrocyte glycoprotein (MOG35–55) induced experimental autoimmune encephalomyelitis (EAE) in C57BL/6 mice, J Vis Exp (2014), doi:10.3791/51275.

18. Calvier L, Demuth G, Manouchehri N, Wong C, Sacharidou A, Mineo C, Shaul PW, Monson NL, Kounnas MZ, Stüve O, Herz J, Reelin depletion protects against autoimmune encephalomyelitis by decreasing vascular adhesion of leukocytes, Sci. Transl. Med. 12, eaay7675 (2020). [PubMed: 32801146]

19. Calvier L, Xian X, Lee RG, Sacharidou A, Mineo C, Shaul PW, Kounnas MZ, Tsai S, Herz J, Reelin Depletion Protects Against Atherosclerosis by Decreasing Vascular Adhesion of Leukocytes, Arterioscler Thromb Vasc Biol 41, 1309–1318 (2021). [PubMed: 33626909]

20. Lin Z, Jin J, Bai W, Li J, Shan X, Netrin-1 prevents the attachment of monocytes to endothelial cells via an anti-inflammatory effect, Mol. Immunol. 103, 166–172 (2018). [PubMed: 30290313]

21. Ly NP, Komatsuzaki K, Fraser IP, Tseng AA, Prodhan P, Moore KJ, Kinane TB, Netrin-1 inhibits leukocyte migration in vitro and in vivo, Proc. Natl. Acad. Sci. U.S.A. 102, 14729–14734 (2005). [PubMed: 16203981]

22. Calvier L, Chouvarine P, Legchenko E, Hoffmann N, Geldner J, Borchert P, Jonigk D, Mozes MM, Hansmann G, PPARγ Links BMP2 and TGFβ1 Pathways in Vascular Smooth Muscle Cells, Regulating Cell Proliferation and Glucose Metabolism, Cell Metab. 25, 1118–1134.e7 (2017). [PubMed: 28467929]

23. Calvier L, Boucher P, Herz J, Hansmann G, LRP1 Deficiency in Vascular SMC Leads to Pulmonary Arterial Hypertension That Is Reversed by PPARγ Activation, Circ. Res. 124, 1778–1785 (2019). [PubMed: 31023188]

24. Calvier L, Chouvarine P, Legchenko E, Kokeny G, Mozes MM, Hansmann G, Chronic TGF-β1 Signaling in Pulmonary Arterial Hypertension Induces Sustained Canonical Smad3 Pathways in Vascular Smooth Muscle Cells, Am. J. Respir. Cell Mol. Biol. 61, 121–123 (2019). [PubMed: 31259625]
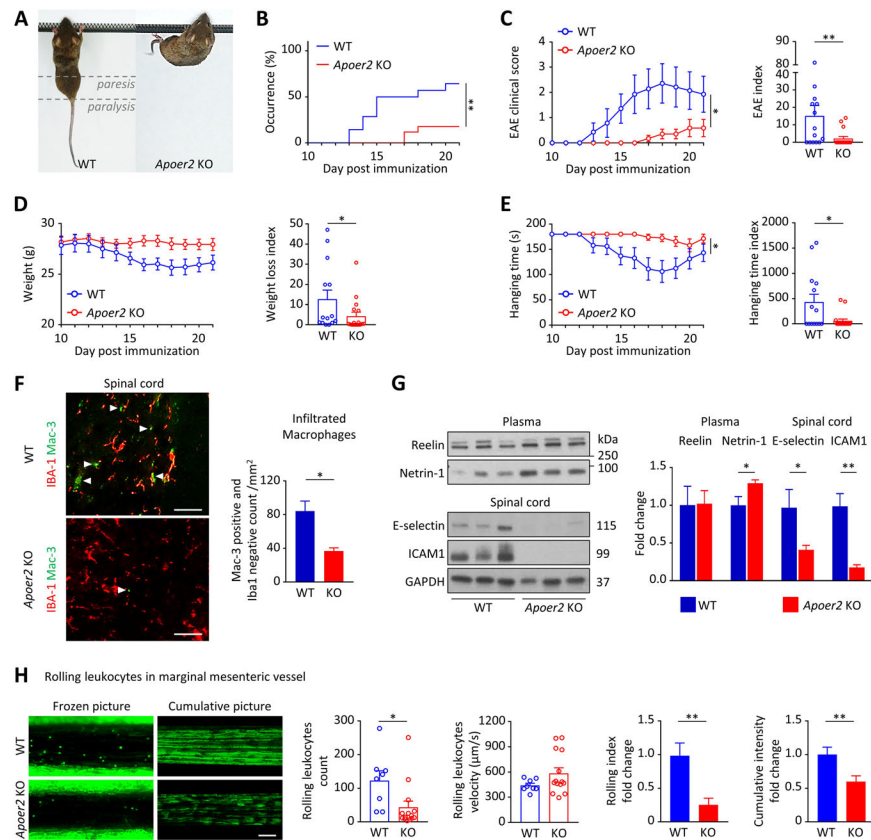
Figure 1. ApoER2 deletion protects mice from EAE by reducing leukocyte recruitment.
A, EAE was induced by MOG immunization in 8 weeks old ApoER2 WT (n=14) and KO (n=17) male littermates (the experiment was performed twice and the results were pooled). **B**, Disease incidence (clinical signs of paralysis) was monitored daily for 21 days. **C-E**, EAE severity was evaluated daily from day 10 using (**C**) an EAE clinical score (from 0=unaffected to 10=dead), (**D**) weight loss and (**E**) inverted hanging test (for a maximum time of 180 sec). **C-E**, EAE severity, weight loss and hanging time indices were calculated for each animal by integrating daily scores over the course of the experiment. **F**, In the spinal cord, the total number of infiltrating macrophages (Mac-3-positive, Iba-1-negative; indicated by the arrows) was evaluated by immunofluorescence (scale = 50 μm). **G**, 21 days after EAE induction, expression of Reelin and Netrin-1 in the plasma, as well as E-selectin and ICAM-1 in the spinal cord were measured by immunoblotting. **H**, 4-week-old ApoER2 WT (n=8) and KO (n=14) male and female littermates received Rhodamine 6G by retro-orbital injection to label circulating leukocytes. Next, intravital microscopy was performed to record numbers and speed of rolling leucocytes on marginal mesenteric vessels. 6 different vessels/mouse were recorded for 10 sec and analyzed; cumulative pictures represent individual images (100 frames/second) integrated over a 10 sec period and stacked; rolling index = leucocyte number / velocity. *p<0.05 and **p<0.01 (Mantel-Cox test, 2-way ANOVA or t-test / Mann Whitney).
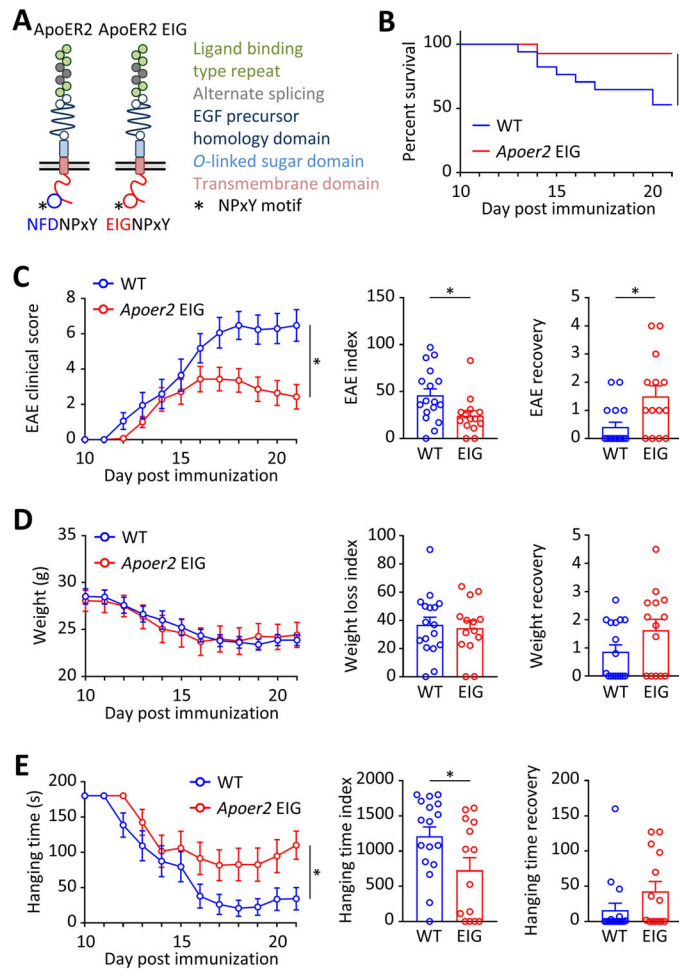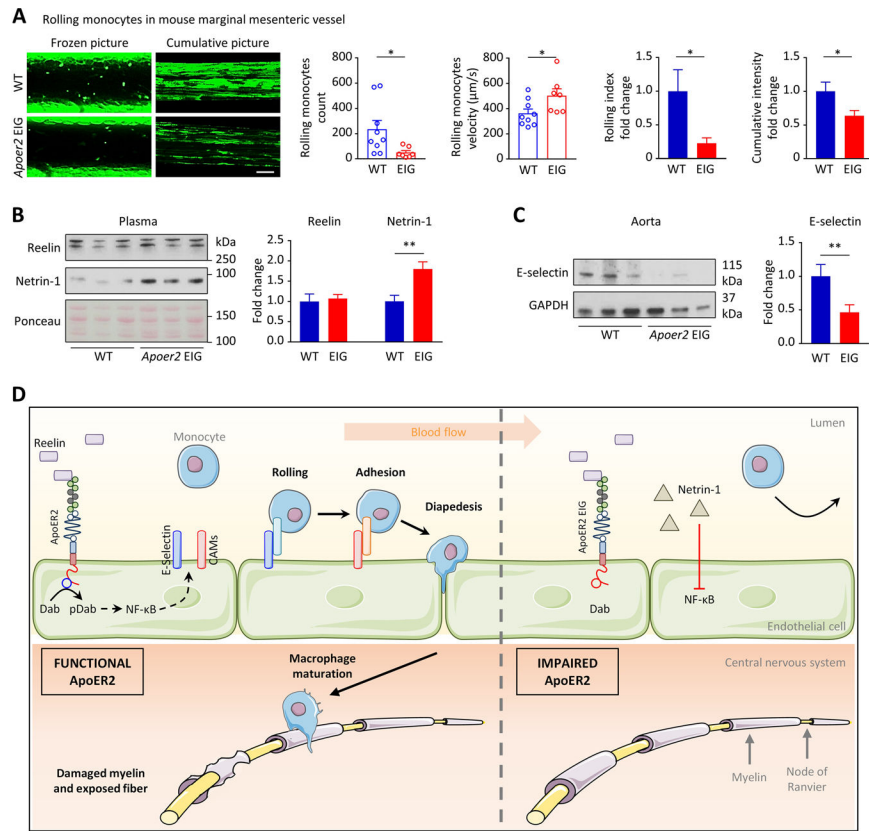
Figure 2. Impaired ApoER2 function in mice reduces EAE severity.

A, We used ApoER2-EIG mutant mice in which the ApoER2 NFDNPVY docking motif for Dab1/2 was rendered non-functional to disrupt the ApoER2-Dab interaction, thereby impairing ApoER2 signaling and function. This line was crossed to *Cx3cr1-GFP* mice expressing GFP in monocytes to follow the infiltration of this specific inflammatory cell population. **B-G**, EAE was induced by MOG immunization in 8 weeks old ApoER2 WT (n=17) and EIG (n=14) male littermates. **B-E**, EAE severity was scored daily starting at day 10 by recording (**B**) survival, (**C**) EAE clinical score (from 0=unaffected to 10=dead), (**D**) weight loss and (**E**) inverted grid hanging endurance (for a maximum time of 180 sec). **C-E**, EAE severity, weight loss and hanging time indices are calculated for each animal by integrating daily scores over the course of the experiment. *p<0.05 and **p<0.01 (Mantel-Cox test, 2-way ANOVA or t-test / Mann Whitney).
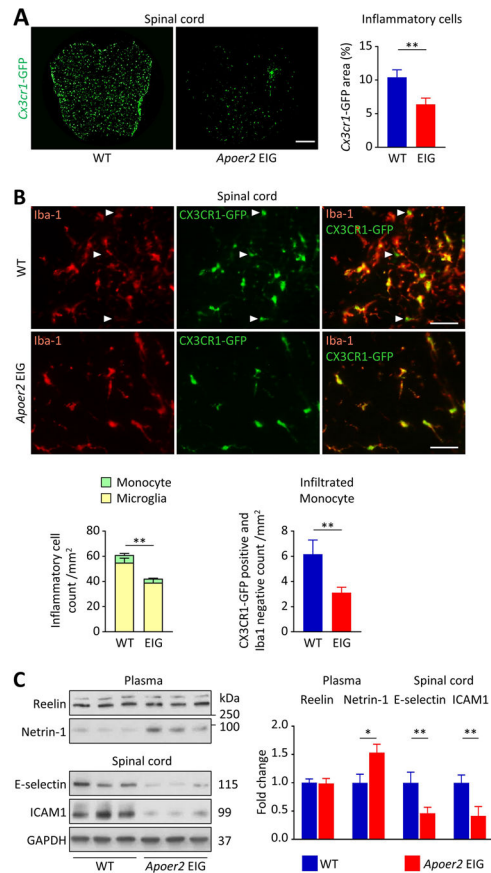
Figure 3. Impaired ApoER2 function in mice reduces monocyte infiltration into the CNS.
A-C, Tissues from WT and ApoER2-EIG mutant mice were analyzed 21 days after
EAE induction. **A**, *Cx3cr1*-GFP fluorescence area was quantified in spinal cord (scale =
200μm). **B**, In the *Cx3cr1*-GFP-positive cell population, the total number of inflammatory
cells (*Cx3cr1*-GFP-positive), monocytes (*Cx3cr1*-GFP-positive, Iba-1-negative; indicated
by the arrows) and microglia (*Cx3cr1*-GFP and Iba1 double positive) were visualized by
immunofluorescence (scale = 50μm). Bar graphs represent the cell population average per
group. **C**, Expression of Reelin and Netrin-1 in the plasma as well as E-selectin and ICAM-1
in the spinal cord were measured by immunoblotting. *p<0.05 and **p<0.01 (t-test / Mann
Whitney).

Figure 4. Impaired ApoER2 function in mice reduces endothelial-monocyte adhesion.
A, Intravital microscopy was performed on 4-week-old ApoER2 WT (n=9) and EIG (n=7) male and female littermates to record numbers and speed of rolling monocytes in marginal mesenteric vessels. 6 different vessels/mouse were recorded for 10 sec and analyzed; cumulative pictures represent individual images (100 frames/second) integrated over a 10 sec period and stacked; rolling index = monocyte number/velocity. **B,C**, After intravital microscopy, immunoblotting was performed on plasma and aorta protein extracts. *p<0.05 and **p<0.01 (t-test/Mann Whitney). **D**, Mechanistic model incorporating the findings described in this article and the literature to date, as discussed. ApoER2 promotes the expression of vascular adhesion proteins, thereby increasing monocyte adhesion/extravasation, inflammation and consequently demyelination. Both ApoER2 deletion or loss of function prevent this inflammatory cascade and thus paralysis in a murine EAE model. We surmise that the same mechanism is conserved in humans suggesting a novel, non-immunosuppressive, therapeutic approach to a broad spectrum of inflammatory diseases.